Technische Universität Berlin
Institut für Mathematik

# 2nd Order Shape Optimization using Wavelet BEM

K. Eppler and H. Harbrecht[1]

[1] TU Chemnitz, Faculty of mathematics

Preprint 2003/06

Preprint-Reihe des Instituts für Mathematik
Technische Universität Berlin

Report 2003/06 June 2003

This present paper is concerned with second order methods for a class of shape optimization problems. We employ a complete boundary integral representation of the shape Hessian which involves first and second order derivatives of the state and the adjoint state function, as well as normal derivatives of its local shape derivatives. We introduce a boundary integral formulation to compute these quantities. The derived boundary integral equations are solved efficiently by a wavelet Galerkin scheme. A numerical example validates that, in spite of the higher effort of the Newton method compared to first order algorithms, we obtain more accurate solutions in less computational time. **AMS subject classification:** 49Q10, 65N38

# 2ND ORDER SHAPE OPTIMIZATION USING WAVELET BEM

K. EPPLER AND H. HARBRECHT

Abstract. This present paper is concerned with second order methods for a class of shape optimization problems. We employ a complete boundary integral representation of the shape Hessian which involves first and second order derivatives of the state and the adjoint state function, as well as normal derivatives of its local shape derivatives. We introduce a boundary integral formulation to compute these quantities. The derived boundary integral equations are solved efficiently by a wavelet Galerkin scheme. A numerical example validates that, in spite of the higher effort of the Newton method compared to first order algorithms, we obtain more accurate solutions in less computational time.

## Introduction

In Eppler and Harbrecht [12] we considered first order algorithms for elliptic shape optimization problems with additional functional constraints, where we proposed the boundary element method (BEM) for the computation of shape gradients and the objective value. In the present paper we extend the approach to second order methods. As we have already mentioned in the introduction of [12], this requires a complete boundary integral representation of all shape derivatives appearing in the algorithms. We emphasize that these quantities have to be computed on different domains a lot of times during the optimization algorithm. Here, the application of boundary elements for the discretization requires only a partition of the boundary. Consequently, no triangulation of the domain is needed like for finite elements.

Nevertheless, the corresponding system matrices are densely populated in general for boundary element methods. Therefore, the complexity for solving such equations grows at least quadratic with the number of equations. This fact restricts the maximal size of the linear equations seriously. Modern methods for the fast solution of BEM reduce the complexity to a suboptimal rate or even an optimal rate, that is a linear rate. Prominent examples for such methods are the *fast multipole method* by Greengard and Rokhlin [14] and the *panel clustering* by Hackbusch and Novack [16]. Observed first by Beylkin, Coifman and Rokhlin [2], the *wavelet Galerkin scheme*

*Date*: March 2003.

*Key words and phrases.* shape optimization, boundary element method, multiscale methods, augmented Lagrangian approach, Newton method.

offers another tool for the fast solution of integral equations. In fact, as proven by Dahmen, Harbrecht and Schneider [6, 17, 20, 27], the wavelet Galerkin scheme for the fast solution of boundary integral equations produces approximate solutions within discretization error accuracy offered by the underlying Galerkin method at a computational expense that stays proportional to the number of unknowns. As it is shown in [12], this results in powerful first order shape optimization algorithms.

Of course, the Newton method requires a complete boundary integral formulation for the shape Hessian, which can be found for example in [9]. However, such expressions contain not only first order normal derivatives of the state and the adjoint state on the boundary, but also second order spatial derivatives and the normal derivative of the related local shape derivatives. Consequently, more effort has to be spent to perform the computations *completely on the boundary*. In particular, we utilize a commutator approach with respect to the tangential differentiation to derive second order derivatives, proposed by Schulz, Schwab and Wendland [28, 29]. As we show in the present paper, invoking suitable Newton potentials, the knowledge of first order and second order normal and tangential derivatives suffices to evaluate the data appearing from the state functions. Besides of problems with net generation and computational complexity, standard FEM will have difficulties for the realization of similar computations.

Instead of the Laplacian, our method applies also for the Stokes, Helmholtz or Lamé equation etc., that are all boundary value problems where a fundamental solution is known explicitly. Then, we can formulate our state equation as a boundary integral equation. Especially, we can treat shape optimization problems for exterior boundary value problems as well as obstacle identification problems, cf. [24, 25]. Moreover, we give a precise characterization of the class of objectives for the shape problems, where our strategy can be realized completely straightforward. For the underlying shape calculus we use a simple boundary variational approach as in [12], which is the substructure for constructing the boundary update in the optimization process. For the sake of brevity, we do not list all the approaches for the description of domain or boundary variations. Moreover, for applications and further numerical methods, we refer to the monographs Pironneau [26], Haslinger and Neitaanmäki [21] and Sokolowski and Zolesio [30] and the references therein. We carry out the numerical tests for the Newton method for some shape problems from planar elasticity, where the stationary domains are given analytically by Banichuk and Karihaloo in [1].

The paper is organized as follows. Section 1 is dedicated to the modeling and the second order shape calculus. By discretizing the boundary of the underlying domain we transform the infinite dimensional optimization problem to a finite dimensional one. In Section 2 we introduce the boundary integral formulation for the solution of the state function, the adjoint state function and the corresponding local shape derivatives. We propose a wavelet Galerkin scheme in order to solve the derived boundary integral equations within optimal complexity. At the end of this section we state error estimates with respect to the quantities involved in the optimization process. In Section 3 we present numerical results in comparison to first order algorithms, which confirm the theory as well as – despite of the effort for computing the shape Hessian – the power of the second order algorithm.

## 1. First and Second order shape calculus

1.1. **The model problem.** Let $\Upsilon$ denote the set of all bounded domains $\Omega \in C^{2,\alpha}$, $\Omega \subseteq D \subseteq \mathbb{R}^2$, starshaped with respect to $B_\delta(\mathbf{0})$. The outer security set $D \subseteq \mathbb{R}^2$ (the *hold all* set) is simply connected and closed, but not necessarily bounded. We consider the following shape optimization problem

$$J(\Omega) = \int_\Omega h(\mathbf{x})u(\mathbf{x}) + h_0(\mathbf{x})d\mathbf{x} = \min_{\Omega\in\Upsilon} \tag{1.1}$$

subject to

$$\begin{aligned} J_1(\Omega) &= \textstyle\int_\Omega h_1(\mathbf{x})d\mathbf{x} \le c_1, \\ J_2(\Omega) &= \textstyle\int_\Omega h_2(\mathbf{x})d\mathbf{x} \le c_2, \\ &\vdots \\ J_m(\Omega) &= \textstyle\int_\Omega h_m(\mathbf{x})d\mathbf{x} \le c_m, \end{aligned} \tag{1.2}$$

where the state function $u$ solves the Dirichlet boundary value problem

$$\begin{aligned} \Delta u &= f \quad \text{in } \Omega, \\ u &= g \quad \text{on } \Gamma. \end{aligned} \tag{1.3}$$

In order to conceive a well posed problem the functions $f$, $g$, $h$ and $h_0, \ldots, h_m$ are assumed sufficiently regular on the whole set $D$. Constraints of practical interest in shape problems are the volume of a domain ($h_i \equiv 1$) or the unscaled barycentre ($h_i(\mathbf{x}) = x$ and $h_i(\mathbf{x}) = y$). Of course, equality constraints and functionals of t he type (1.1) can be considered as constraints as well. Furthermore, boundary integral constraints of the type

$$J_i(\Omega) = \int_\Gamma h_i(\mathbf{x})d\sigma_{\mathbf{x}} \le c_i,$$

e.g. for the perimeter ($h_i \equiv 1$), can be treated as well. To shorten the presentation, we do not discuss this extension in the present paper. Note, that such constraints will imply a different coercivity behaviour of the shape Hessian of Lagrangian-, Penalty- and Augmented Lagrangian functionals, see [9, 11].

**Remark 1.1.** *Instead of the Laplace equation* (1.3)*, our method applies also for the Stokes or Helmholtz equation etc., that are all boundary value problems where a fundamental solution is known explicitly. Then, we can formulate our state equation as a boundary integral equation. In particular, exterior boundary value problems can be considered as well, cf.* [24, 25].

1.2. **Shape derivatives.** Clearly, the domain $\Omega \in C^{k,\alpha}$ can be identified with a boundary describing function for $\Gamma = \partial\Omega$, i.e., in polar coordinates we have

$$\Gamma := \Big\{\boldsymbol{\gamma}(\phi) = r(\phi)\big[\begin{smallmatrix}\cos\phi\\ \sin\phi\end{smallmatrix}\big] : \phi \in [0, 2\pi]\Big\},$$

where $r \in C^{k,\alpha}_{\text{per}}[0, 2\pi]$ is a positive function with $r > \delta$ and

$$C^{k,\alpha}_{\text{per}}[0, 2\pi] = \{r \in C^{k,\alpha}[0, 2\pi] : r^{(i)}(0) = r^{(i)}(2\pi),\ i = 0(1)k\}. \tag{1.4}$$

As a standard variation for perturbed domains $\Omega_\varepsilon$ and boundaries $\Gamma_\varepsilon$, respectively, we introduce a function $dr \in C^{k,\alpha}_{\text{per}}[0, 2\pi]$

$$r_\varepsilon(\phi) = r(\phi) + \varepsilon dr(\phi),$$

where $\boldsymbol{\gamma}_\varepsilon(\phi) = r_\varepsilon(\phi)\mathbf{e}_r(\phi)$ is always a Jordan curve. Herein, $\mathbf{e}_r(\phi) = [\cos\phi, \sin\phi]^T$ denotes the unit vector in the outer radial direction. The main advantage of this simple approach is a complete embedding of the shape problem into a Banach space setting. That is, *both* the shapes and its increments, can be viewed as elements of $C^{k,\alpha}_{\text{per}}[0, 2\pi]$.

Next, we adopt the general shape calculus to our model problem, cf. [9, 10]. Due to a second order boundary perturbation calculus, we have to assume $\Omega \in C^{2,\alpha}$ for some fixed $\alpha \in (0, 1)$ in contrary to $\Omega \in C^2$ for the first order calculus. The shape gradient of the functional (1.1) has the following boundary integral formulation

$$\nabla J(\Omega)[dr] = \int_\Gamma dr\,\langle \mathbf{e}_r, \mathbf{n}\rangle \bigg\{(hu + h_0) + \frac{\partial p}{\partial \mathbf{n}}\frac{\partial(g-u)}{\partial \mathbf{n}}\bigg\}\,d\sigma,$$

which becomes in polar coordinates

$$\nabla J(\Omega)[dr] = \int_0^{2\pi} dr\,r\,\bigg\{(hu + h_0)\big|_\Gamma + \frac{\partial p}{\partial \mathbf{n}}\frac{\partial(g-u)}{\partial \mathbf{n}}\bigg\}\,d\phi. \tag{1.5}$$

Here, the adjoint state function is defined by

$$\begin{aligned} -\Delta p &= h \quad \text{in } \Omega,\\ p &= 0 \quad \text{on } \Gamma. \end{aligned} \tag{1.6}$$

With respect to the inequality constraints (1.2) one finds

$$\nabla J_i(\Omega)[dr] = \int_\Gamma dr\,\langle \mathbf{e}_r, \mathbf{n}\rangle\,h_i\,d\sigma = \int_0^{2\pi} dr\,r\,h_i\big|_\Gamma d\phi$$

for $i = 1, 2, \ldots, m$.

The complete boundary integral representation of the shape Hessian is given by

$$\nabla^2 J(\Omega)[dr_1, dr_2] = \int_0^{2\pi} dr_1 dr_2 \Bigg\{ \Big[(hg + h_0)\big|_\Gamma - \frac{\partial p}{\partial \mathbf{n}} \frac{\partial (g-u)}{\partial \mathbf{n}}\Big] + r\frac{\partial}{\partial \mathbf{e}_r}\Big[(hg + h_0)\big|_\Gamma - \frac{\partial p}{\partial \mathbf{n}} \cdot \frac{\partial (g-u)}{\partial \mathbf{n}}\Big]\Bigg\} + r\, dr_1 \Big[\frac{\partial p}{\partial \mathbf{n}} \cdot \frac{\partial du[dr_2]}{\partial \mathbf{n}} - \frac{\partial dp[dr_2]}{\partial \mathbf{n}} \cdot \frac{\partial (g-u)}{\partial \mathbf{n}}\Big] d\phi. \tag{1.7}$$

Herein, $du[dr_2]$ and $dp[dr_2]$ denote the local shape derivatives of the state function and the adjoint state function which solve

$$\begin{aligned} \Delta du &= 0 && \text{in } \Omega, \\ du &= dr_2 \,\langle \mathbf{e}_r, \mathbf{n}\rangle \big[\tfrac{\partial g}{\partial \mathbf{n}} - \tfrac{\partial u}{\partial \mathbf{n}}\big] && \text{on } \Gamma, \end{aligned} \tag{1.8}$$

and

$$\begin{aligned} \Delta dp &= 0 && \text{in } \Omega, \\ dp &= -dr_2 \,\langle \mathbf{e}_r, \mathbf{n}\rangle \tfrac{\partial p}{\partial \mathbf{n}} && \text{on } \Gamma, \end{aligned} \tag{1.9}$$

respectively. The shape Hessian of the constraints (1.2) reads

$$\nabla^2 J_i(\Omega)[dr_1, dr_2] = \int_0^{2\pi} dr_1\, dr_2 \Big[h_i\big|_\Gamma + r\frac{\partial h_i}{\partial \mathbf{e}_r}\big|_\Gamma\Big] d\phi$$

for $i = 1, \ldots, m$.

1.3. **Finite dimensional representation of boundaries.** Based on the polar coordinate approach, we can express the smooth function $r \in C^{2,\alpha}_{\text{per}}([0, 2\pi])$ by

$$r(\phi) = a_0 + \sum_{n=1}^{\infty} a_n \cos n\phi + a_{-n} \sin n\phi.$$

Hence, the truncated Fourier series

$$r_N(\phi) = a_0 + \sum_{n=1}^{N} a_n \cos n\phi + a_{-n} \sin n\phi.$$

provides a reasonable approximation of $r$, defining the finite dimensional setting. We mention that also other boundary description like B-splines can be considered as well.

The advantages of our approach is an exponential convergence if the shape is analytical, i.e.,

$$\|r - r_N\|_{L^\infty([0,2\pi])} \lesssim q^N \tag{1.10}$$

for an appropriate $q < 1$. Additionally, the approximation $r_N$ is analytical which makes the application of the wavelet Galerkin scheme for the boundary element method much more efficient [20].

Consequently, for the domain functionals $J_i(\Omega) = \int_\Omega h_i(\mathbf{x})d\mathbf{x}$, the shape gradient as well as the Hessian are approximated by the truncated Fourier series

$$\nabla_N J_i(\Omega) := \int_0^{2\pi} \begin{bmatrix} \sin N\phi \\ \sin(N-1)\phi \\ \vdots \\ \cos N\phi \end{bmatrix} \cdot r(\phi)\, h_i(\phi)\, d\phi,$$

$$\nabla_N^2 J(\Omega) := \int_0^{2\pi} \begin{bmatrix} \sin N\phi \\ \sin(N-1)\phi \\ \vdots \\ \cos N\phi \end{bmatrix} \begin{bmatrix} \sin N\phi \\ \sin(N-1)\phi \\ \vdots \\ \cos N\phi \end{bmatrix}^T \cdot \Big[h_i(\phi) + r(\phi)\frac{\partial h_i}{\partial \mathbf{e}_r}(\phi)\Big] d\phi.$$

This approximation is directly feasible for the shape gradient $\nabla J$ (1.5) of the objective and for the first term of the shape Hessian $\nabla^2 J$ (1.7) with the leading term $dr_1 dr_2$, provided that the spatial first and second order derivatives of $u$ and $p$ are computed. In the last term of the shape Hessian, the direction $dr_2$ is involved in the Dirichlet-to-Neumann map for the local shape derivatives $du$ and $dp$, respectively. Hence, for computing one row of the approximated shape Hessian, we have to solve these maps for each basis function. Note that this structure implies the $H^{1/2}$-coercivity of $\nabla^2 J$.

## 2. Boundary integral formulation

2.1. **Newton potentials.** During an iterative optimization process, we have to solve the boundary value problems (1.3), (1.6), (1.8) and (1.9) in each step. We emphasize that the underlying domains are always different. Finite element methods suffer from generating a suitable triangulation for each new domain. One way out is to reformulate the given boundary value problems into boundary integral equations since only functions living on the boundary have to be discretized. In order to perform this reformulation, we suppose Newton potentials $N_f$ and $N_h$ satisfying

$$\Delta N_f = f, \qquad \Delta N_h = h, \qquad \text{in } \widehat{\Omega}, \tag{2.11}$$

where $\widehat{\Omega}$ is a sufficiently large domain containing all domains from the iteration process. These Newton potentials are supposed to be explicitly known like in our numerical example (Section 3) or computed with sufficiently high accuracy. Such an idea is proposed for example by Jung and Steinbach [22]. It turns out in the subsequent subsections that we require these potentials as well as their gradients and Hessians. Therefore, one cannot compute them only by globally continuous finite elements. But since the domain $\widehat{\Omega}$ can be chosen fairly simple, one can use, for example, finite elements based on tensor products of higher order B-splines (in $[-R, R]^2$) or dual reciprocity methods. The ansatz

$$u = N_f + v, \qquad p = N_h + q, \tag{2.12}$$

yields the problem of seeking harmonic functions $v$ and $q$ satisfying

$$\begin{aligned} \Delta v &= 0, & \Delta q &= 0, & &\text{in } \Omega,\\ v &= g - N_f, & q &= -N_h, & &\text{on } \Gamma. \end{aligned} \tag{2.13}$$

Now, these boundary value problems can be reformulated by boundary integral equations. For the sake of brevity we concentrate ourselves to the first problem since the second one is treated in complete analogy.

2.2. **Evaluation of the functional.** At first glance the evaluation of $\int_\Omega h\,u\,d\mathbf{x}$ seems to require the explicit knowledge of the state function $u$ on the complete domain $\Omega$. But inserting $v := N_h$ into Green's second formula

$$\int_\Omega u\Delta v\,d\mathbf{x} = \int_\Omega \Delta uv\,d\mathbf{x} + \int_\Gamma u\frac{\partial v}{\partial \mathbf{n}}\,d\sigma - \int_\Gamma \frac{\partial u}{\partial \mathbf{n}}v\,d\sigma,$$

and observing $\Delta u = f$, $u\big|_\Gamma = g$ as well as $\Delta N_h = h$, we derive the equation

$$\int_\Omega u\,h\,d\mathbf{x} = \int_\Omega N_h\,f\,d\mathbf{x} + \int_\Gamma g\,\frac{\partial N_h}{\partial \mathbf{n}}\,d\sigma - \int_\Gamma \frac{\partial u}{\partial \mathbf{n}}\,N_h\,d\sigma. \tag{2.14}$$

Note that the volume integral can be computed easily by exploiting polar coordinates. Hence, we are able to compute the functional $J(\Omega)$ only with the knowledge of the normal derivative of the state function.

**Remark 2.1.** *If the Newton potential $N_h$ is known analytically this volume integral can be transformed to a boundary integral by exploiting polar coordinates and performing the integration over the angle $\phi$. If $N_h$ is approximated numerically, one has indeed to evaluate this volume integral by quadrature rules.*

2.3. **First order derivatives.** Now we discuss the computation of the first order derivatives $\frac{\partial u}{\partial \mathbf{t}}$ and $\frac{\partial u}{\partial \mathbf{n}}$. Of course, the first one is simply computed by

$$\frac{\partial u}{\partial \mathbf{t}} = \frac{\partial g}{\partial \mathbf{t}}, \tag{2.15}$$

i.e., without explicit knowledge of the state function $u$.

With respect to the normal derivative of $u$, we obtain from the ansatz (2.12) the equation

$$\frac{\partial u}{\partial \mathbf{n}} = \frac{\partial v}{\partial \mathbf{n}} + \frac{\partial N_f}{\partial \mathbf{n}}. \tag{2.16}$$

Herein, the normal derivative of $v$ can be solved by a boundary integral equation. We introduce the *single layer operator* $\mathcal{V}$ and the *double layer operator* $\mathcal{K}$ defined by

$$\begin{aligned} (\mathcal{V}u)(\mathbf{x}) &:= -\frac{1}{2\pi}\int_\Gamma \log\|\mathbf{x}-\mathbf{y}\|u(\mathbf{y})d\sigma_{\mathbf{y}},\\ (\mathcal{K}u)(\mathbf{x}) &:= \frac{1}{2\pi}\int_\Gamma \frac{\langle \mathbf{n}_{\mathbf{y}}, \mathbf{x}-\mathbf{y}\rangle}{\|\mathbf{x}-\mathbf{y}\|^2}u(\mathbf{y})d\sigma_{\mathbf{y}}. \end{aligned}$$

Then, the normal derivative of $v$ is given by the Dirichlet-to-Neumann map

$$\mathcal{V}\frac{\partial v}{\partial \mathbf{n}} = \Big(\frac{1}{2}+\mathcal{K}\Big)(g-N_f). \tag{2.17}$$

We denote the function space of all squared integrable functions on $\Gamma$ with respect to the canonical inner product

$$(u,v)_{L^2(\Gamma)} = \int_\Gamma uv\, d\sigma$$

by $L^2(\Gamma)$ and the associated Sobolev spaces by $H^s(\Gamma)$, $s\in\mathbb{R}$. Then, in this context, $\mathcal{V}: H^{-1/2}(\Gamma)\to H^{1/2}(\Gamma)$ defines an operator of the order $-1$ while $\frac{1}{2}+\mathcal{K}: H^{1/2}(\Gamma)\to H^{1/2}(\Gamma)$ defines an operator of the order 0.

According to the definition of the gradient (1.5) of our functional the knowledge of these first order derivatives are sufficient to perform a first order optimization method. But the computation of the Hessian (1.7) requires also second order derivatives.

2.4. **Second order derivatives.** In this section we calculate $\frac{\partial^2 u}{\partial \mathbf{t}^2}$, $\frac{\partial^2 u}{\partial \mathbf{n}\partial \mathbf{t}}$ and $\frac{\partial^2 u}{\partial \mathbf{n}^2}$. The first and third quantities can be computed directly from known derivatives as we show in the next lemma.

**Lemma 2.2.** *There hold the identities*

$$\frac{\partial^2 u}{\partial \mathbf{t}^2} = +\frac{\partial^2 g}{\partial \mathbf{t}^2} + \kappa\left(\frac{\partial v}{\partial \mathbf{n}} - \frac{\partial(g-N_f)}{\partial \mathbf{n}}\right),$$
$$\frac{\partial^2 u}{\partial \mathbf{n}^2} = -\frac{\partial^2 g}{\partial \mathbf{t}^2} - \kappa\left(\frac{\partial v}{\partial \mathbf{n}} - \frac{\partial(g-N_f)}{\partial \mathbf{n}}\right) + f,$$

*where $\kappa$ denotes the curvature of $\Gamma$.*

*Proof.* We have to prove that

$$\frac{\partial^2 v}{\partial \mathbf{t}^2} = +\frac{\partial^2 (g-N_f)}{\partial \mathbf{t}^2} + \kappa\left(\frac{\partial v}{\partial \mathbf{n}} - \frac{\partial(g-N_f)}{\partial \mathbf{n}}\right),$$
$$\frac{\partial^2 v}{\partial \mathbf{n}^2} = -\frac{\partial^2 (g-N_f)}{\partial \mathbf{t}^2} - \kappa\left(\frac{\partial v}{\partial \mathbf{n}} - \frac{\partial(g-N_f)}{\partial \mathbf{n}}\right).$$

To this end, let $\gamma:[0,L]\to\Gamma$ denote a regular parametric representation of the boundary $\Gamma$. Then, we obtain the formulas

$$\mathbf{t}(s) = \frac{\gamma'(s)}{\|\gamma'(s)\|}, \quad \kappa(s) = -\frac{\langle \gamma''(s), \mathbf{n}(s)\rangle}{\|\gamma'(s)\|^2}.$$

From

$$\begin{aligned}\frac{\partial^2 v}{\partial s^2} &= \frac{\partial}{\partial s}\langle \nabla v, \gamma' \rangle \\ &= \langle \langle \nabla^2 v, \gamma' \rangle, \gamma' \rangle + \langle \nabla v, \gamma'' \rangle \\ &= \|\gamma'\|^2 \frac{\partial^2 v}{\partial \mathbf{t}^2} + \langle \gamma'', \mathbf{t} \rangle \frac{\partial v}{\partial \mathbf{t}} + \langle \gamma'', \mathbf{n} \rangle \frac{\partial v}{\partial \mathbf{n}}\end{aligned}$$

we conclude that

$$\frac{\partial^2 v}{\partial \mathbf{t}^2} = \frac{1}{\|\gamma'\|^2}\frac{\partial^2 v}{\partial s^2} - \frac{\langle \gamma'', \mathbf{t} \rangle}{\|\gamma'\|^2}\frac{\partial v}{\partial \mathbf{t}} - \frac{\langle \gamma'', \mathbf{n} \rangle}{\|\gamma'\|^2}\frac{\partial v}{\partial \mathbf{n}}. \tag{2.18}$$

Now, in the derivate with respect to the parameter $s$, we replace $v$ by the boundary conditions $g - N_f$

$$\frac{\partial^2 v}{\partial s^2} = \|\gamma'\|^2 \frac{\partial^2 (g - N_f)}{\partial \mathbf{t}^2} + \langle \gamma'', \mathbf{t} \rangle \frac{\partial (g - N_f)}{\partial \mathbf{t}} + \langle \gamma'', \mathbf{n} \rangle \frac{\partial (g - N_f)}{\partial \mathbf{n}}.$$

Inserting this relation into (2.18) yields the first assertion. The second assertion follows immediately from

$$\frac{\partial^2 v}{\partial \mathbf{t}^2} + \frac{\partial^2 v}{\partial \mathbf{n}^2} = \Delta v = 0.$$

□

Next, we have to compute $\frac{\partial^2 u}{\partial \mathbf{n} \partial \mathbf{t}}$. Due to (2.12) we find

$$\frac{\partial^2 u}{\partial \mathbf{n} \partial \mathbf{t}} = \frac{\partial^2 v}{\partial \mathbf{n} \partial \mathbf{t}} + \frac{\partial^2 N_f}{\partial \mathbf{n} \partial \mathbf{t}}$$

with the unknown function $\frac{\partial^2 v}{\partial \mathbf{n} \partial \mathbf{t}}$. It is advantageous to choose a boundary integral formulation since we do not loose the regularity of $\frac{\partial u}{\partial \mathbf{n}}$. This formulation can be motivated as follows. Given a boundary integral operator $(\mathcal{A}u)(\mathbf{x}) = \int_\Gamma k(\mathbf{x}, \mathbf{y}) u(\mathbf{y}) d\sigma_\mathbf{y}$ and a regular parametrization $\gamma : [0, L] \to \Gamma$, we find the equation

$$\begin{aligned}0 = \int_0^L & k\big(\gamma(s), \gamma(t)\big) \|\gamma'(t)\| \frac{\partial u}{\partial \mathbf{t}}\big(\gamma(t)\big) dt \\ &+ \int_0^L \frac{\partial}{\partial \mathbf{t}(t)} \big[k\big(\gamma(s), \gamma(t)\big) \|\gamma'(t)\|\big] u\big(\gamma(t)\big) dt.\end{aligned}$$

Consequently, the tangential derivatative of $\mathcal{A}u$ is given by

$$\begin{aligned}\frac{\partial (\mathcal{A}u)}{\partial \mathbf{t}}\big(\gamma(s)\big) &= \int_0^L \frac{\partial}{\partial \mathbf{t}(s)} \big[k\big(\gamma(s), \gamma(t)\big) \|\gamma'(t)\|\big] u\big(\gamma(t)\big) dt \\ &= \int_0^L \Big(\frac{\partial}{\partial \mathbf{t}(s)} + \frac{\partial}{\partial \mathbf{t}(t)}\Big) \big[k\big(\gamma(s), \gamma(t)\big) \|\gamma'(t)\|\big] u\big(\gamma(t)\big) dt \\ &\qquad + \int_0^L k\big(\gamma(s), \gamma(t)\big) \|\gamma'(t)\| \frac{\partial u}{\partial \mathbf{t}}\big(\gamma(t)\big) dt \\ &= \Big(\Big[\mathcal{A}, \frac{\partial}{\partial \mathbf{t}}\Big] u\Big)\big(\gamma(s)\big) + \Big(\mathcal{A} \frac{\partial u}{\partial \mathbf{t}}\Big)\big(\gamma(s)\big).\end{aligned}$$

The operator $\big[\mathcal{A},\frac{\partial}{\partial\mathbf{t}}\big]$ denotes the commutator of $\mathcal{A}$ and defines an operator of identical order as $\mathcal{A}$, cf. [28, 29].

Differentiation of (2.17) with respect to the tangent and application of the above manipulation yields the boundary integral equation

$$\mathcal{V}\frac{\partial^2 v}{\partial\mathbf{n}\partial\mathbf{t}} = \Big(\frac{1}{2}+\mathcal{K}\Big)\frac{\partial(g-N_f)}{\partial\mathbf{t}} + \Big[\frac{1}{2}+\mathcal{K},\frac{\partial}{\partial\mathbf{t}}\Big](g-N_f) - \Big[\mathcal{V},\frac{\partial}{\partial\mathbf{t}}\Big]\frac{\partial v}{\partial\mathbf{n}}. \tag{2.19}$$

The commutators with respect to the single and double layer operator are of the order $-1$ and $0$, respectively, that is

$$\begin{aligned}\big[\mathcal{V},\tfrac{\partial}{\partial\mathbf{t}}\big] &: H^{-1/2}(\Gamma)\to H^{1/2}(\Gamma),\\ \big[\tfrac{1}{2}+\mathcal{K},\tfrac{\partial}{\partial\mathbf{t}}\big] &: H^{1/2}(\Gamma)\to H^{1/2}(\Gamma).\end{aligned}$$

They are given by

$$\begin{aligned}\Big(\Big[\mathcal{V},\frac{\partial}{\partial\mathbf{t}}\Big]u\Big)(\gamma(s)) = -\frac{1}{2\pi}\int_0^L \bigg\{&\frac{\langle\gamma(s)-\gamma(t),\mathbf{t}(s)-\mathbf{t}(t)\rangle}{\|\gamma(s)-\gamma(t)\|^2}\|\gamma'(t)\|\\ &+\log\|\gamma(s)-\gamma(t)\|\frac{\langle\gamma''(t),\mathbf{t}(t)\rangle}{\|\gamma'(t)\|}\bigg\}u(t)dt\end{aligned}$$

and

$$\begin{aligned}\Big(\Big[\frac{1}{2}+\mathcal{K},\frac{\partial}{\partial\mathbf{t}}\Big]u\Big)(\gamma(s)) = \frac{1}{2\pi}\int_0^L \bigg\{&\frac{\langle\mathbf{t}(s),\mathbf{n}(t)\rangle}{\|\gamma(s)-\gamma(t)\|^2}\|\gamma'(t)\|\\ &-\frac{\langle\gamma(s)-\gamma(t),\mathbf{t}(t)\rangle\langle\gamma''(t),\mathbf{n}(t)\rangle}{\|\gamma(s)-\gamma(t)\|^2}+\frac{\langle\gamma(s)-\gamma(t),\mathbf{n}(t)\rangle\langle\gamma''(t),\mathbf{t}(t)\rangle}{\|\gamma(s)-\gamma(t)\|^2}\\ &-2\frac{\langle\gamma(s)-\gamma(t),\mathbf{n}(t)\rangle\langle\gamma(s)-\gamma(t),\mathbf{t}(s)-\mathbf{t}(t)\rangle}{\|\gamma(s)-\gamma(t)\|^4}\|\gamma'(t)\|\bigg\}u(t)dt.\end{aligned}$$

2.5. **The wavelet Galerkin scheme.** Boundary element methods provide a common tool for the solution of boundary integral equations. In general, cardinal B-splines are used as ansatz functions in the Galerkin formulation. But discretizing the boundary integral equations (2.17) and (2.19) with respect to such *single-scale bases* yields densely populated system matrices. In combination with the ill-posedness of the single layer operator and its commutator, this implies at least a quadratic complexity for their solution. The crucial idea of the wavelet Galerkin scheme is a change of bases, i.e., applying appropriate (biorthogonal) wavelet bases instead of the traditional single-scale bases. Then, the arising system matrices become quasi-sparse and can be compressed without loss of accuracy, cf. [18, 19, 20, 27].

For a fixed domain, we have to solve the boundary integral equations (2.17) and (2.19) several times, namely,

- the Dirichlet-to-Neumann map (2.17) applies to the state function, the adjoint state function and the associated local shape derivatives, while
- (2.19) has to be evaluated for the state function and the adjoint state function.

Hence, an efficient realization discretizes both, the boundary integral operators on the left *and* right hand side of the given boundary integral equations. This requires a mixed formulation in order to achieve the optimal order of convergence. For the sake of simplicity we consider in the present paper only the case of piecewise constant and linear functions.

Exploiting polar coordinates, we introduce a parametrical representation of the boundary in accordance with

$$\gamma : [0,1] \to \Gamma, \quad s \mapsto \gamma(s) := r(2\pi s)\left[\begin{smallmatrix}\cos(2\pi s)\\ \sin(2\pi s)\end{smallmatrix}\right].$$

We subdivide the boundary $\Gamma$ into $2^l$ panels $\pi_{l,k} := \gamma\big(2^{-l}[k,k+1)\big)$, where $k \in \triangle_l := \{0,1,\ldots,2^l-1\}$. We denote the space of the piecewise constants and linears defined on the given partition by $V_l^{(1)} = \operatorname{span}\Phi_l^{(1)}$ and $V_l^{(2)} = \operatorname{span}\Phi_l^{(2)}$. Herein, a single function of the collection $\Phi_l^{(d)} := \{\phi_{l,k}^{(d)} : k \in \triangle_l\}$ is given via

$$\phi_{l,k}^{(1)} = 2^{l/2}\chi_{\pi_{l,k}}.$$

and

$$\phi_{l,k}^{(2)}(\mathbf{x}) = 2^{3l/2}\begin{cases} s - 2^{-l}(k-1), & \mathbf{x} = \gamma(s) \in \pi_{l,k-1},\\ 2^{-l}(k+1) - s, & \mathbf{x} = \gamma(s) \in \pi_{l,k},\\ 0, & \text{elsewhere,}\end{cases}$$

respectively. Note that we use a $L^2$-normalization, i.e., $\|\phi_{l,k}^{(d)}\|_{L^2(\Gamma)} \sim 1$ for $d = 1,2$.

The two sequences of nested spaces

$$V_{l_0}^{(d)} \subset V_{l_0+1}^{(d)} \subset \ldots \subset L^2(\Gamma),$$

generate a multiscale analysis, cf. [3]. We introduce suitable wavelet bases $\Psi_l^{(d)} := \{\psi_{l,k}^{(d)} : k \in \triangle_l\}$ which span complementary spaces $W_l^{(d)} := \operatorname{span}\Psi_l^{(d)}$ with

$$V_l^{(d)} \oplus W_l^{(d)} = V_{l+1}^{(d)}.$$

For the matrix compression, these wavelet bases are required to provide *vanishing moments* in terms of

$$\int_\Gamma \big(\gamma^{-1}(\mathbf{x})\big)^\alpha \psi_{l,k}^{(d)}(\mathbf{x})d\sigma = 0, \quad 0 \le \alpha < \widetilde{d}.$$

According to [18, 19], it suffices to consider piecewise constant wavelets with $\widetilde{d} = 3$ vanishing moments and piecewise linear wavelets with $\widetilde{d} = 2$ vanishing moments.

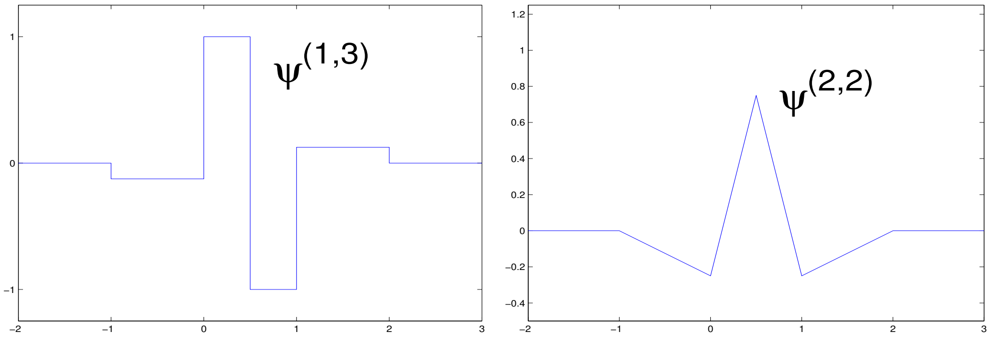


FIGURE 2.1. Piecewise constant and linear functions respective wavelets.

Such wavelets have been constructed in [3]. They can be characterized by their refinement relation

$$\psi_{l,k}^{(d)} = \sum_j a_j \phi_{l+1,2k+j}^{(d)}$$

via the *mask coefficients*

$$\begin{aligned} (a_{-2}, a_{-1}, \ldots, a_3) &= (-1/8, -1/8, 1, -1, 1/8, 1/8), \qquad d = 1, \\ (a_{-1}, a_0, \ldots, a_3) &= (-1/8, -1/4, 3/4, -1/4, -1/8), \quad d = 2, \end{aligned}$$

cf. Figure 2.1. It is well known [3] that the collections

$$\Psi_L^{(d)} := \bigcup_{l=l_0-1}^{L-1} \Psi_l^{(d)}, \qquad \Psi_{l_0-1}^{(d)} := \Phi_{l_0}^{(d)},$$

form uniformly stable bases in $L^2(\Gamma)$. In fact, this *Riesz property* implies the existence of a corresponding *dual* multiresolution analysis. We refer to [3, 20, 27] for details.

We make the ansatz $\frac{\partial v}{\partial \mathbf{n}} = \Psi_L^{(1)} \mathbf{v}_L$ and $\frac{\partial^2 v}{\partial \mathbf{n} \partial \mathbf{t}} = \Psi_L^{(1)} \widetilde{\mathbf{v}}_L$. Then, introducing the system matrices

$$\begin{aligned} \mathbf{V}_L &:= (\mathcal{V}\Psi_L^{(1)}, \Psi_L^{(1)})_{L^2(\Gamma)}, & \widetilde{\mathbf{V}}_L &:= \big(\big[\mathcal{V}, \tfrac{\partial}{\partial \mathbf{t}}\big]\Psi_L^{(1)}, \Psi_L^{(1)}\big)_{L^2(\Gamma)}, \\ \mathbf{K}_L &:= \big((\tfrac{1}{2} + \mathcal{K})\Psi_L^{(2)}, \Psi_L^{(1)}\big)_{L^2(\Gamma)}, & \widetilde{\mathbf{K}}_L &:= \big(\big[\tfrac{1}{2} + \mathcal{K}, \tfrac{\partial}{\partial \mathbf{t}}\big]\Psi_L^{(2)}, \Psi_L^{(1)}\big)_{L^2(\Gamma)}, \end{aligned} \tag{2.20}$$

the data vectors

$$\mathbf{u}_L := (g - N_f, \Psi_L^{(2)})_{L^2(\Gamma)}, \quad \widetilde{\mathbf{u}}_L := \big(\tfrac{\partial (g - N_f)}{\partial \mathbf{t}}, \Psi_L^{(2)}\big)_{L^2(\Gamma)}$$

and the mass matrix

$$\mathbf{G}_L := (\Psi_L^{(2)}, \Psi_L^{(2)})_{L^2(\Gamma)},$$

the boundary integral equation (2.17) corresponds to

$$\mathbf{V}_L \mathbf{v}_L = \mathbf{K}_L \big(\mathbf{G}_L\big)^{-1} \mathbf{u}_L,$$

while (2.19) corresponds to

$$\mathbf{V}_L\widetilde{\mathbf{v}}_L = \mathbf{K}_L\big(\mathbf{G}_L\big)^{-1}\widetilde{\mathbf{u}}_L + \widetilde{\mathbf{K}}_L\big(\mathbf{G}_L\big)^{-1}\mathbf{u}_L + \widetilde{\mathbf{V}}_L\mathbf{v}_L.$$

Consequently, we have to compute only four system matrices for each new domain, but solving the discrete systems several times with different data vectors. We mention that $\big(\mathbf{G}_L\big)^{-1}\mathbf{u}_L\Psi_L^{(d)}$ and $\big(\mathbf{G}_L\big)^{-1}\widetilde{\mathbf{u}}_L\Psi_L^{(d)}$ denote the $L^2$-othogonal projections onto $V_L^{(2)}$ of the given data $g - N_f$ and $\frac{\partial(g-N_f)}{\partial\mathbf{t}}$, respectively.

As mentioned above, the system matrices (2.20) are quasi-sparse. They can be compressed without loss of accuracy to $\mathcal{O}(2^L)$ nonvanishing matrix entries, see [18, 20, 27] for details. Actually, in accordance with [17, 20, 27], the over-all complexity of compressing and assembling the system matrices is still asymptotically linear. Moreover, based on the well known norm equivalences of wavelet bases, $\operatorname{diag}(\mathbf{V}_L^{\psi})$ and $\operatorname{diag}(\widetilde{\mathbf{V}}_L^{\psi})$ provide simple (diagonal) preconditioner for the given boundary integral equations [5, 7, 27]. We like to stress that, besides the difficulties of the net generation and the computation of second order derivatives, modern finite element method have the complexity $\mathcal{O}(2^{2L})$.

2.6. **Error estimates.** In this subsection we state error estimates. For this, we consider a fixed domain and sufficiently smooth data. Our estimates are based on the following crucial lemma.

**Lemma 2.3.** *We assume that the Newton potentials $N_f$ is given exactly. Then, denoting by $\overline{\frac{\partial v}{\partial\mathbf{n}}}$ and $\overline{\frac{\partial^2 v}{\partial\mathbf{n}\partial\mathbf{t}}}$ the approximations of $\frac{\partial v}{\partial\mathbf{n}}$ and $\frac{\partial^2 v}{\partial\mathbf{n}\partial\mathbf{t}}$, respectively, we obtain the error estimates*

$$\left\|\frac{\partial v}{\partial\mathbf{n}} - \overline{\frac{\partial v}{\partial\mathbf{n}}}\right\|_{H^s(\Gamma)} \lesssim 2^{L(s-1)}, \qquad \left\|\frac{\partial^2 v}{\partial\mathbf{n}\partial\mathbf{t}} - \overline{\frac{\partial^2 v}{\partial\mathbf{n}\partial\mathbf{t}}}\right\|_{H^s(\Gamma)} \lesssim 2^{L(s-1)}, \tag{2.21}$$

*for all $-2 \le s < 1/2$. In case of applicating (2.17) to the local shape derivative $du[dr]$ defined by (1.8), we obtain*

$$\left\|\frac{\partial du[dr]}{\partial\mathbf{n}} - \overline{\frac{\partial du[dr]}{\partial\mathbf{n}}}\right\|_{H^s(\Gamma)} \lesssim 2^{L(s-1)}, \tag{2.22}$$

*for all $-1 \le s < 1/2$.*

*Proof.* The first error estimate (2.21) is an immediate consequence of the traditional error analysis of the Galerkin scheme.

The second estimate is derived as follows. The Dirichlet data of (1.8) are of the type $p - q\frac{\partial v}{\partial\mathbf{n}}$ with smooth functions $p, q, \frac{\partial v}{\partial\mathbf{n}}$. Hence, (2.22) follows immediately if $\frac{\partial v}{\partial\mathbf{n}}$ is given analytically. But, since the latter one is available only as piecewise constant approximation, we have to prove that the additional consistency error satisfies

$$\left\| \left(p - q\frac{\partial v}{\partial \mathbf{n}}\right) - Q_L\left(p - q\overline{\frac{\partial v}{\partial \mathbf{n}}}\right)\right\|_{L^2(\Gamma)} \lesssim 2^{-2L},$$

where $Q_L : L^2(\Gamma) \to V_L^{(2)}$ denotes the orthogonal projection onto $V_L^{(2)}$.

We make use of the following result from [4]. Denoting the midpoints of the panels $\pi_{L,k}$ by $\mathbf{m}_{L,k} := \gamma\big(2^{-L}(k + 1/2)\big)$, we find the estimate

$$\sup_{k\in\triangle_L} \left| \left(\frac{\partial v}{\partial \mathbf{n}} - \overline{\frac{\partial v}{\partial \mathbf{n}}}\right)(\mathbf{m}_{L,k})\right| \lesssim 2^{-2L}.$$

Next, defining for sufficiently smooth $p \in L^2(\Gamma)$ its interpolate $J_L p$ as the unique $J_L p \in V_L^{(2)}$ such that

$$(J_L p)\big(\gamma(2^{-L}k)\big) := \big\{p(\mathbf{m}_{L,k-1}) + p(\mathbf{m}_{L,k})\big\}/2,$$

we arrive at

$$\left\| \left(p - q\frac{\partial v}{\partial \mathbf{n}}\right) - J_L\left(p - q\overline{\frac{\partial v}{\partial \mathbf{n}}}\right)\right\|_{L^2(\Gamma)} \lesssim 2^{-2L}.$$

Since $Q_L$ ist the orthogonal projection onto $V_L^{(2)}$, we deduce

$$\left\| \left(p - q\frac{\partial v}{\partial \mathbf{n}}\right) - Q_L\left(p - q\overline{\frac{\partial v}{\partial \mathbf{n}}}\right)\right\|_{L^2(\Gamma)} \le \left\| \left(p - q\frac{\partial v}{\partial \mathbf{n}}\right) - J_L\left(p - q\overline{\frac{\partial v}{\partial \mathbf{n}}}\right)\right\|_{L^2(\Gamma)} \lesssim 2^{-2L}.$$

□

The next lemma invokes also approximation errors with respect to the Newton potentials.

**Lemma 2.4.** *We assume that the numerically computed Newton potential $\overline{N_f}$ satisfies the pointwise estimates*

$$\|N_f - \overline{N_f}\|_{L^\infty(\widehat{\Omega})} \lesssim 2^{-3L},$$
$$\|\nabla N_f - \overline{\nabla N_f}\|_{L^\infty(\widehat{\Omega})} \lesssim 2^{-3L},$$
$$\|\nabla^2 N_f - \overline{\nabla^2 N_f}\|_{L^\infty(\widehat{\Omega})} \lesssim 2^{-2L}.$$

*Then, there holds*

$$\left\| \frac{\partial u}{\partial \mathbf{n}} - \overline{\frac{\partial u}{\partial \mathbf{n}}}\right\|_{H^s(\Gamma)} \lesssim 2^{L(s-1)} \tag{2.23}$$

*for all $-2 \le s \le 0$, as well as*

$$\left\| \frac{\partial^2 u}{\partial \mathbf{n}\partial \mathbf{t}} - \overline{\frac{\partial^2 u}{\partial \mathbf{n}\partial \mathbf{t}}}\right\|_{H^s(\Gamma)} \lesssim 2^{L(s-1)}, \qquad \left\| \frac{\partial du[dr]}{\partial \mathbf{n}} - \overline{\frac{\partial du[dr]}{\partial \mathbf{n}}}\right\|_{H^s(\Gamma)} \lesssim 2^{L(s-1)}. \tag{2.24}$$

*for all $-1 \le s \le 0$.*

*Proof.* Treating the approximation errors of the Newton potentials as error of quadrature, the estimates (2.23) and (2.24) are an immediate consequence of the estimates of the previous lemma. □

**Theorem 2.5.** *Let the assumptions of the previous lemma hold. Then, the order of convergence with respect to the gradient* (1.5) *and the Hessian* (1.7) *is quadratic while the order of convergence of the functional itself* (1.1) *is cubic, that is*

$$\begin{aligned} |J(\Omega) - \overline{J(\Omega)}| &\lesssim 2^{-3L}, \\ |\nabla J[dr](\Omega) - \overline{\nabla J[dr](\Omega)}| &\lesssim 2^{-2L}, \\ |\nabla^2 J[dr_1, dr_2](\Omega) - \overline{\nabla^2 J[dr_1, dr_2](\Omega)}| &\lesssim 2^{-2L}. \end{aligned}$$

*Proof.* We prove first the cubic order of convergence with respect to the functional. We find

$$\begin{aligned} |(N_h - \overline{N_h}, f)_{L^2(\Omega)}| &\lesssim \|N_h - \overline{N_h}\|_{L^\infty(\widehat{\Omega})} \|f\|_{L^1(\Omega)} \lesssim 2^{-3L}, \\ \Big|\Big(\tfrac{\partial N_h}{\partial \mathbf{n}} - \overline{\tfrac{\partial N_h}{\partial \mathbf{n}}}, g\Big)_{L^2(\Gamma)}\Big| &\lesssim \|\nabla N_h - \nabla \overline{N_h}\|_{L^\infty(\widehat{\Omega})} \|g\|_{L^1(\Gamma)} \lesssim 2^{-3L}. \end{aligned}$$

Moreover,

$$\begin{aligned} &\Big|\Big(\tfrac{\partial u}{\partial \mathbf{n}} - \overline{\tfrac{\partial u}{\partial \mathbf{n}}}, N_h - \overline{N_h}\Big)_{L^2(\Gamma)}\Big| \\ &\quad \le \Big|\Big(\tfrac{\partial v}{\partial \mathbf{n}} + \tfrac{\partial N_f}{\partial \mathbf{n}} - \overline{\tfrac{\partial v}{\partial \mathbf{n}}} - \overline{\tfrac{\partial N_f}{\partial \mathbf{n}}}, N_h - \overline{N_h}\Big)_{L^2(\Gamma)}\Big| \\ &\quad \lesssim \Big\{\Big\|\tfrac{\partial v}{\partial \mathbf{n}} - \overline{\tfrac{\partial v}{\partial \mathbf{n}}}\Big\|_{L^2(\Gamma)} + \|\nabla N_h - \overline{\nabla N_h}\|_{L^\infty(\widehat{\Omega})}\Big\} \|N_h - \overline{N_h}\|_{L^\infty(\widehat{\Omega})} \\ &\quad \lesssim 2^{-4L}. \end{aligned}$$

Hence, in accordance with (2.14) we conclude

$$|J(\Omega) - \overline{J(\Omega)}| \lesssim 2^{-3L}.$$

Considering smooth functions $f$, $g$ and $h$ and approximations $\overline{g}$ and $\overline{h}$ with

$$\|g - \overline{g}\|_{H^s(\Gamma)} \lesssim 2^{L(s-1)}, \qquad \|h - \overline{h}\|_{H^s(\Gamma)} \lesssim 2^{L(s-1)}$$

for all $-1 \le s \le 0$, we conclude from the identity

$$gh - \overline{g}\overline{h} = g(h - \overline{h}) + h(g - \overline{g}) - (g - \overline{g})(h - \overline{h})$$

that

$$
\begin{aligned}
&|(f, gh - \overline{g}\overline{h})_{L^2(\Gamma)}| \\
&\qquad \le \big|\big(fg, (h - \overline{h})\big)_{L^2(\Gamma)}\big| + \big|\big(fh, (g - \overline{g})\big)_{L^2(\Gamma)}\big| + \big|\big(f, (g - \overline{g})(h - \overline{h})\big)_{L^2(\Gamma)}\big| \\
&\qquad \le \|fg\|_{H^1(\Gamma)}\|h - \overline{h}\|_{H^{-1}(\Gamma)} + \|fh\|_{H^1(\Gamma)}\|g - \overline{g}\|_{H^{-1}(\Gamma)} \\
&\qquad\qquad + \|f\|_{L^\infty(\Gamma)}\|g - \overline{g}\|_{L^2(\Gamma)}\|h - \overline{h}\|_{L^2(\Gamma)}\big\} \\
&\qquad \lesssim 2^{-2L}.
\end{aligned}
$$

Using this argument, the proofs of the remaining orders of convergence are straightforward. □

## 3. Test example, optimization methods and numerical results

3.1. **The test problem and penalization of constraints.** For comparison reasons we employ a model problem where the optimal shape is known analytically. We consider a cylindric circular bar which is homogeneous and isotropic with a planar, simply connected cross section $\Omega \in \mathbb{R}^2$. We follow Banichuk and Karihaloo [1] but normalize the shear modulus $G = 1$ and the elastic modulus $E = 1$. We want to solve the problem of maximizing the torsional rigidity of the bar subject to given inequality constraints on the stiffness rigidity and the volume. In [12] first order algorithms have been introduced for the solution of this problem.

First, we briefly recall the mathematical formulation of the quantities. Moreover, we give the related expressions in polar coordinates, if this is explicitly possible. The torsional rigidity is calculated by

$$T(\Omega) = 2\int_\Omega u(\mathbf{x})d\mathbf{x} = 2\int_0^{2\pi}\int_0^{r(\phi)} u(\rho,\phi)\,\rho d\rho d\phi.$$

Thus, since we want to maximize the torsional rigidity, we have $h \equiv -2$ and $h_0 \equiv 0$ in (1.1). The stress function $u = u(\Omega)$ satisfies

$$
\begin{aligned}
\Delta u &= -2 \quad \text{in } \Omega, \\
u &= 0 \qquad \text{on } \Gamma.
\end{aligned}
$$

The adjoint state function is defined identically, i.e., $p = u$. We find the explicit Newton potentials $N_f = N_h = \frac{1}{2}(x^2 + y^2)$.

The bending rigidity with respect to a fixed barycentre in the origin is given by

$$B(\Omega) = \int_\Omega y^2 d\mathbf{x} = \frac{1}{4}\int_0^{2\pi} \sin^2\phi r^4(\phi)d\phi.$$

The volume of the domain and its (simplified) barycentre coordinates read as

$$V(\Omega) = \int_\Omega d\mathbf{x} = \frac{1}{2}\int_0^{2\pi} r^2(\phi)d\phi,$$
$$\begin{bmatrix}\widehat{x}_b(\Omega)\\ \widehat{y}_b(\Omega)\end{bmatrix} = \int_\Omega \mathbf{x}d\mathbf{x} = \int_0^{2\pi}\begin{bmatrix}\cos\phi\\ \sin\phi\end{bmatrix} r^3(\phi)d\phi.$$

These quantities define the functionals $J_1(\Omega), \ldots, J_4(\Omega)$.

In [12] we considered both for the penalization of the constraints, a standard quadratic penalty functional for inequality constraints as well as the Augmented Lagrangian method for equality constraints. Since the penalty functional is not sufficiently smooth and less efficient, we compare in the following only the results of the Augmented Lagrangian approach

$$\begin{aligned} L_c(\Omega, \boldsymbol{\lambda}) = -T(\Omega) + \lambda_B\big(B(\Omega) - B_0\big) + \lambda_V\big(V(\Omega) - V_0\big) + \lambda_{\widehat{x}_b}\widehat{x}_b(\Omega) + \lambda_{\widehat{y}_b}\widehat{y}_b(\Omega)\\ + \frac{c}{2}\Big[\big(T(\Omega) - T_0\big)^2 + \big(V(\Omega) - V_0\big)^2 + \widehat{x}_b(\Omega)^2 + \widehat{y}_b(\Omega)^2\Big]\end{aligned}$$

with first order update for the multiplier $\boldsymbol{\lambda} = (\lambda_B, \lambda_V, \lambda_{\widehat{x}_b}, \lambda_{\widehat{y}_b})$. For further details concerning the optimization we refer to [8, 13, 15] and the references therein.

Due to the efficiency of the Newton method with respect to the inner iteration, from our experiences, the first order Lagrange multiplier update becomes the bottleneck for the optimization algorithm. Mårtensson proposed in [23] a second order method where the multiplier is viewed as a function of the original variables, i.e. $\boldsymbol{\lambda} = \boldsymbol{\lambda}(\Omega)$. In fact, this yields a faster convergence close to the optimal shape. But for sake of fairness in the comparison of first and second order optimization algorithms we restrict our numerical considerations to the first order update of the Lagrange multipliers.

3.2. **Numerical results.** In Table 3.2 we list the absolute errors of the approximations with respect to the functional. The underlying domain is an ellipse which is approximated via 33 Fourier coefficients ($N = 16$). As reference solution we take the solution on the level $L = 14$, that is $2^L = 16384$ boundary elements. We compute the gradient as vector and the Hessian as matrix with respect to all Fourier coefficients in accordance with subsection 1.3. Their tabulated absolute errors are measured with respect to the associated Euclidean norms. The bracketed values indicate the ratio of the previous error and the present error. A cubic order of convergence implies a ratio of 8 while for a quadratic order the ratio should be close to four. One figures out of Table 3.2 the expected rates of convergence, i.e., a cubic order with respect to the functional and quadratic orders with respect to the gradient and the Hessian. The last column of Table 3.2 contains the over-all computing times (in seconds) to derive the measured quantities. We mention that the expected complexity is linear since the volume integral in (2.14) can be transformed to a boundary integral, cf. [12] for the details. Unfortunately, the ascent of the computing times is only nearly linear. We suppose that this results from cache-based effects of the computer. But let us remark that we compute four system matrices and solve two linear systems on the level $L = 13$ in only five minutes.

| $L$ | $2^L$ | $\lvert J(\Omega) - \overline{J(\Omega)}\rvert$ | $\lVert\nabla J(\Omega) - \overline{\nabla J(\Omega)}\rVert$ | $\lVert\nabla^2 J(\Omega) - \overline{\nabla^2 J(\Omega)}\rVert$ | cpu-time |
|---|---|---|---|---|---|
| 5 | 32 | 1.6e-05 | 2.1e-03 | 1.16 | 0.3 |
| 6 | 64 | 1.6e-06 (10) | 3.7e-04 (5.8) | 1.0e-01 (11) | 0.8 |
| 7 | 128 | 2.0e-07 (8.1) | 9.4e-06 (3.9) | 8.3e-03 (12) | 1.7 |
| 8 | 256 | 2.1e-08 (9.2) | 2.4e-06 (4.0) | 8.7e-04 (9.6) | 3.9 |
| 9 | 512 | 4.4e-09 (4.8) | 6.0e-07 (4.0) | 1.3e-04 (6.7) | 9.4 |
| 10 | 1024 | 3.8e-10 (11) | 1.5e-07 (4.0) | 3.3e-05 (3.9) | 22 |
| 11 | 2048 | 3.0e-11 (12) | 3.7e-08 (4.1) | 8.3e-06 (4.0) | 54 |
| 12 | 4096 | 3.0e-11 (1.0) | 8.9e-09 (4.2) | 2.0e-06 (4.2) | 125 |
| 13 | 8192 | 8.9e-13 (33) | 1.7e-09 (5.2) | 4.0e-07 (5.0) | 306 |

TABLE 3.1. Absolute errors of approximation and over-all computing times.

Table 3.2 is concerned with the comparison of a first order optimization iteration (Quasi-Newton method updated by the inverse BFGS-rule without damping) and the Newton scheme. We tabulate the absolute $l^2$-errors of the Fourier coefficients of the optimal shape and their approximation computed by these schemes. We choose the number $N = 16$ of Fourier coefficients fixed but vary the number of boundary elements. Let us remark that in order to increase the region of convergence of the Newton scheme we perform first quasi-Newton steps until the gradient becomes sufficiently small. Then, we switch to the Newton method.

| $L$ | $2^L$ | Quasi-Newton method | Newton method |
|---|---|---|---|
| 6 | 64 | 1.3e-04 | 1.8e-05 |
| 7 | 128 | 1.0e-03 | 6.6e-06 |
| 8 | 256 | 3.1e-04 | 2.3e-06 |
| 9 | 512 | 1.6e-05 | 1.0e-06 |
| 10 | 1024 | 1.9e-06 | 2.1e-07 |
| 11 | 2048 | 1.1e-06 | 7.8e-08 |
| 12 | 4096 | 9.3e-07 | 6.2e-08 |

TABLE 3.2. Approximation errors $\|r - r_N\|$ of the shapes.

In the last table (Table 3.2) we investigate the speed-up achieved by the Newton method in comparison with the quasi-Newton method. For ten randomly chosen domains we perform the optimization process with both schemes until an error of approximation less than 1e-3 to the optimal shape. The tabulated numbers denote the means of our measurement. One figures out that the Newton method requires less than half the number of approximate PDE-solutions compared to the quasi-Newton method while the speed-up is 33%. In the Newton scheme, the solution of the underlying partial differential equation is more expensive due to the computation of higher order derivatives. But we observed that the update established by the Newton scheme makes a line search nearly obsolete.

| Quasi-Newton method | | Newton method | |
|---|---|---|---|
| PDE-solutions | cpu-time | PDE-solutions | cpu-time |
| 54.0 | 70 | 22.6 | 47.7 |

TABLE 3.3. Numbers of PDE-solutions and cpu-times to achieve an error of approximation less than 1e-3.

## References


[1] N.V. Banichuk and B.L. Karihaloo. Minimum-weight design of multi-purpose cylindrical bars. *International Journal of solids and Structures*, 12:267–273, 1976.

[2] G. Beylkin, R. Coifman, and V. Rokhlin. The fast wavelet transform and numerical algorithms. *Comm. Pure and Appl. Math.*, 44:141–183, 1991.

[3] A. Cohen, I. Daubechies, and J.-C. Feauveau. Biorthogonal bases of compactly supported wavelets. *Pure Appl. Math.*, 45:485–560, 1992.

[4] M. Crouzeix and F.-J. Sayas. Asymptotic expansions of the error of spline Galerkin boundary element methods. *Numer. Math.*, 78:523–547, 1998.

[5] W. Dahmen. Wavelet and multiscale methods for operator equations. *Acta Numerica*, 6:55–228, 1997.

[6] W. Dahmen, H. Harbrecht and R. Schneider. Compression techniques for boundary integral equations – optimal complexity estimates. *Preprint SFB 393/02-06, TU Chemnitz*, 2002. submitted to SIAM J. Numer. Anal.

[7] W. Dahmen and A. Kunoth. Multilevel preconditioning. *Numer. Math.*, 63:315–344, 1992.

[8] J.E. Dennis and R.B. Schnabel. *Numerical Methods for Nonlinear Equations and Unconstrained Optimization Techniques.* Prentice-Hall, Englewood Cliffs, 1983.

[9] K. Eppler. Boundary integral representations of second derivatives in shape optimization. *Discussiones Mathematicae (Differential Inclusion Control and Optimization)*, 20:63–78, 2000.

[10] K. Eppler. Optimal shape design for elliptic equations via BIE-methods. *J. of Applied Mathematics and Computer Science*, 10:487–516, 2000.

[11] K. Eppler. Second derivatives and sufficient optimality conditions for shape functionals. *Control and Cybernetics*, 29:485–512, 2000.

[12] K. Eppler and H. Harbrecht. Numerical solution of elliptic shape optimization problems using wavelet-based BEM. *Optim. Methods Softw.*, 18:105-123, 2003.

[13] A.V. Fiacco and G.P. McCormick. *Nonlinear Programming: Sequential Unconstrained Minimization Techniques*. Wiley, New York, 1968.

[14] L. Greengard and V. Rokhlin. A fast algorithm for particle simulation. *J. Comput. Phys.*, 73:325–348, 1987.

[15] Ch. Grossmann and J. Terno. *Numerik der Optimierung*. Teubner, Stuttgart, 1993.

[16] W. Hackbusch and Z.P. Nowak. On the fast matrix multiplication in the boundary element method by panel clustering. *Numer. Math.*, 54:463–491, 1989.

[17] H. Harbrecht. Wavelet Galerkin schemes for the boundary element method in three dimensions. *PHD Thesis, Technische Universität Chemnitz, Germany*, 2001.

[18] H. Harbrecht, F. Paiva, C. Pérez, and R. Schneider. Biorthogonal wavelet approximation for the coupling of FEM-BEM. *Numer. Math.*, 92:325–356, 2002.

[19] H. Harbrecht, F. Paiva, C. Pérez, and R. Schneider. Wavelet preconditioning for the coupling of FEM-BEM. *Preprint SFB 393/00-07, TU Chemnitz*, 2000. to appear in Numerical Linear Algebra with Applications.

[20] H. Harbrecht and R. Schneider. Wavelet Galerkin Schemes for 2D-BEM. In *Operator Theory: Advances and Applications*, volume 121. Birkhäuser, (2001).

[21] J. Haslinger and P. Neitaanmäki. *Finite Element Approximation for Optimal Shape, Material and Topological Design, 2nd edition*. Wiley, Chichester, 1996.

[22] M. Jung and O. Steinbach. A Finite Element-Boundary Element Algorithm for Inhomogeneous Boundary Value Problems *Computing*, 68:1–17, 2002.

[23] K. Mårtensson (1973) A new approach to constrained function optimization. *J. of Optimization Theory and Application*. 12: 531–554.

[24] A. Novruzi Contribution en Optimisation des Formes et Applications. PHD Thesis, Nancy, 1997.

[25] M. Pierre and J.-R. Roche Computation of free surfaces in the electromagnetic shaping of liquid metals by optimization algorithms. *Eur. J. Mech*, 10: 489–500, 1991.

[26] O. Pironneau. *Optimal Shape Design for Elliptic Systems*. Springer, New York, 1983.

[27] R. Schneider. *Multiskalen- und Wavelet-Matrixkompression: Analysisbasierte Methoden zur Lösung großer vollbesetzter Gleichungssyteme*. B.G. Teubner, Stuttgart, 1998.

[28] H. Schulz, C. Schwab and W.L. Wendland. An extraction technique for boundary element methods. In W. Hackbusch and G. Wittum, editors, *Boundary Elements: Implementation and Analysis of Advanced Algorithms*, pages 219–231, 1996.

[29] C. Schwab and W.L. Wendland. On the extraction technique in boundary integral equations. *Math. Comp.*, 68:91–122, 1999.

[30] J. Sokolowski and J.-P. Zolesio. *Introduction to Shape Optimization*. Springer, Berlin, 1992.

Institut für Mathematik, Technische Universität Berlin, 10623 Berlin, Germany.

*E-mail address*: eppler@math.tu-berlin.de

Fakultät für Mathematik, Technische Universität Chemnitz, 09107 Chemnitz, Germany.

*E-mail address*: helmut.harbrecht@mathematik.tu-chemnitz.de